Since January 2020 Elsevier has created a COVID-19 resource centre with free information in English and Mandarin on the novel coronavirus COVID-19. The COVID-19 resource centre is hosted on Elsevier Connect, the company's public news and information website.

ACADEMIC PRESS

Available online at www.sciencedirect.com

SCIENCE DIRECT®

VIROLOGY

Virology 312 (2003) 25–34

www.elsevier.com/locate/yviro

The cytoplasmic tails of infectious bronchitis virus E and M proteins mediate their interaction

Emily Corse and Carolyn E. Machamer*

Department of Cell Biology, The Johns Hopkins University School of Medicine, 725 North Wolfe Street, Baltimore, MD 21205, USA

Received 12 December 2002; returned to author for revision 22 January 2003; accepted 31 January 2003

Abstract

Virus-like particle (VLP) formation by the coronavirus E and M proteins suggests that interactions between these proteins play a critical role in coronavirus assembly. We studied interactions between the infectious bronchitis virus (IBV) E and M proteins using in vivo crosslinking and VLP assembly assays. We show that IBV E and M can be crosslinked to each other in IBV-infected and transfected cells, indicating that they interact. The cytoplasmic tails of both proteins are important for this interaction. We also examined the ability of the mutant and chimeric E and M proteins to form VLPs. IBV M proteins that are missing portions of their cytoplasmic tails or transmembrane regions were not able to support VLP formation, regardless of their ability to be crosslinked to IBV E. Interactions between the E and M proteins and the membrane bilayer are likely to play an important role in VLP formation and virus budding.

Keywords: Coronavirus; Infectious bronchitis virus; Enveloped virus assembly; Virus-like particle

Introduction

Enveloped viruses acquire their lipid membranes from those of the host cell in a process known as budding, in which the virus envelope proteins accumulate at the appropriate membrane and cooperate with the nucleocapsid and other viral components to induce membrane curvature and pinching (Garoff et al., 1998). Most well-studied enveloped viruses, such as influenza and retroviruses, bud from the plasma membrane of cells, which results in the release of virus particles from the host cell as soon as the pinching process is complete. However, the envelopes of other viruses are derived by budding into the lumen of intracellular secretory compartments, such as the endoplasmic reticulum (ER) and Golgi apparatus (Griffiths and Rottier, 1992). Intracellular budding is a seemingly more complex way of obtaining a lipid envelope, since virus particles are contained within intracellular membrane-bound compartments as a result of budding. The newly budded viruses presumably exploit the cellular secretory pathway to exit the cell for a new round of infection. The reasons that some enveloped viruses have evolved to bud inside the cell are not known. Several clinically important viruses bud into intracellular membranes. Viruses of the family *Flaviviridae*, which include hepatitis C virus and Kunjin virus, derive their lipid envelopes by budding into the lumen of the ER (Dubois-Dalcq et al., 1984; Mackenzie and Westaway, 2001). As another example, the hemorrhagic fever-causing Hantaviruses, members of the family *Bunyaviridae*, bud into the membranes of the Golgi complex (Hung et al., 1985; Pettersson, 1991). The advantage provided by intracellular budding remains an interesting and important question in the biology of these and other viruses that obtain their envelopes from intracellular membranes.

Coronaviruses are positive-stranded RNA viruses that acquire their membrane envelope by budding into the lumen of a pre-Golgi compartment or *cis*-Golgi network (CGN) (Klumperman et al., 1994). Accumulating evidence indicates that the E and M proteins are instrumental in this process. Rottier and colleagues made the initial observation that mouse hepatitis virus (MHV) E and M proteins are sufficient to produce membrane-bound particles very similar to virions in size and shape (Vennema et al., 1996), and

* Corresponding author. Fax: +1-410-955-4129.
E-mail address: machamer@jhmi.edu (C.E. Machamer).

0042-6822/03/$ – see front matter © 2003 Elsevier Science (USA). All rights reserved.
doi:10.1016/S0042-6822(03)00175-2

this result has been confirmed with the E and M proteins of several other coronaviruses (Baudoux et al., 1998; Corse and Machamer, 2000; Godeke et al., 2000). These observations suggest that coronavirus budding is directed by envelope proteins alone, which is an unusual type of enveloped virus assembly (Garoff et al., 1998). The coronavirus E protein appears to play a critical role in the budding step, since mutations introduced into the cytoplasmic tail of MHV E by targeted RNA recombination result in elongated virions (Fischer et al., 1998). Indeed, it has been shown that both the MHV E and the infectious bronchitis virus (IBV) E proteins are sufficient for formation of the virus-like particles (VLPs) described above (Corse and Machamer, 2000; Maeda et al., 1999), although the efficiency probably varies with cell type and protein expression system.

We are interested in understanding the mechanisms by which the avian coronavirus IBV selects a bud site and assembles in CGN membranes. We have previously shown that the IBV M and E proteins independently localize to the Golgi region of transfected cells (Corse and Machamer, 2000; Machamer and Rose, 1987) and characterized the Golgi targeting signals in the two proteins that direct this localization (Corse and Machamer, 2002; Machamer et al., 1993). In the study described here, we examined interactions between the IBV E and M proteins in transfected OST7-1 cells using the chemical crosslinker dithiobis[succinimidyl propionate] (DSP). Using mutant E and M proteins that are correctly targeted to the Golgi complex, we found that the cytoplasmic tails of both proteins are required for their interaction. We found that IBV E and M proteins can be efficiently assembled into VLPs in OST7-1 cells, and we investigated which domains of IBV E and M are required for this process. Interestingly, the interaction of M and E, as measured by crosslinking, was not sufficient for VLP formation. It is likely that interactions of E and M with each other as well as the membrane bilayer are important for VLP formation and virus budding.

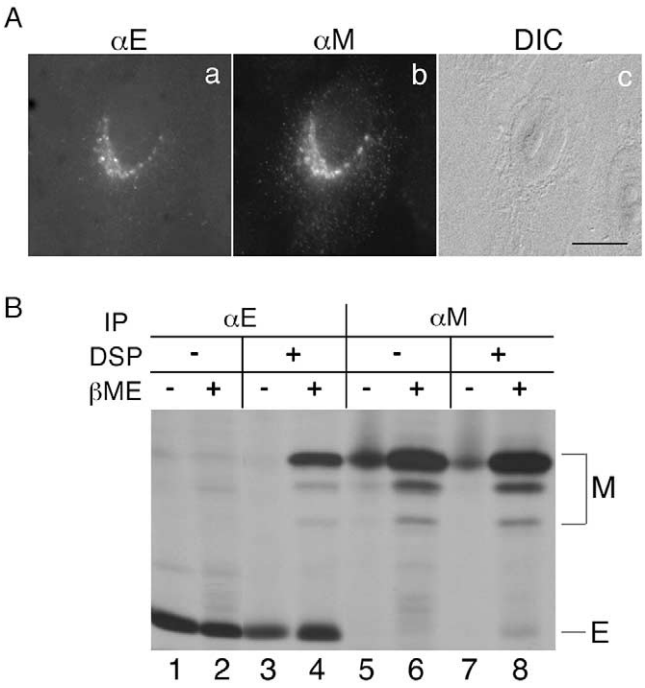

Fig. 1. IBV E and M colocalize and interact in IBV-infected Vero cells. (A) IBV-infected Vero cells were fixed for immunofluorescence at 6 h postinfection and double labeled with rat anti-E antibody (a) and rabbit anti-M antibody (b). Secondary antibodies were fluorescein-conjugated goat anti-rat IgG and Texas red conjugated donkey anti-rabbit IgG. Panel c is a differential interference contrast (DIC) image of the labeled cells. Bar, 15 μm. (B) IBV-infected Vero cells were labeled with [^{35}S]methionine-cysteine at 45 h postinfection, treated with DSP as indicated, lysed, and immunoprecipitated with anti-E or anti-M antibodies as described under Materials and methods. The immunoprecipitates were analyzed by SDS–15% PAGE, in the presence or absence of β-mercaptoethanol (βME) as indicated, and fluorography. IBV E is coprecipitated with IBV M after crosslinking and vice versa. These data are representative of at least three independent experiments.

Results

IBV E and M proteins colocalize in the Golgi region and interact in IBV-infected cells

Although the IBV E protein is distributed throughout the Golgi stack when expressed alone (Corse and Machamer, 2000, 2001), the IBV E and M proteins exactly colocalize in IBV-infected Vero cells examined by indirect immunofluorescence at early times postinfection (Fig. 1A). We wanted to investigate the possibility that this precise colocalization was indicative of a physical interaction between the two proteins. Since attempts to coimmunoprecipitate E and M proteins from IBV-infected Vero cells in a variety of detergent conditions were unsuccessful, we employed the cell-permeable chemical crosslinker DSP, which is a thiol-cleavable molecule that contains two amine-reactive groups separated by a 12 Å spacer arm. IBV-infected Vero cells were radiolabeled at 45 h postinfection and treated with DSP prior to lysis and immunoprecipitation with anti-E or anti-M antibodies. When we analyzed the immunoprecipitates by SDS–PAGE, we found that M was present in the anti-E immunoprecipitations and vice versa (Fig. 1B, lanes 4 and 8). This association was dependent on the presence of DSP since it was not seen in samples that were mock-treated (lanes 2 and 6). Immunoprecipitation with irrelevant antibodies yielded no visible bands (not shown). In the absence of β-mercaptoethanol, which cleaves the disulfide bond of DSP, the unseparated crosslinked E and M proteins were present as high molecular weight aggregates and migrated at a high position on the gel (not shown). The crosslinking and coimmunoprecipitation was not quantitative, since only a fraction of the total E protein (as measured by the amount of E in the anti-E immunoprecipitation) was found in the anti-M immunoprecipitation. This could be due to the inherent inefficiency of chemical crosslinking. Alternatively, this result could reflect the small E:M ratio in virions (Liu

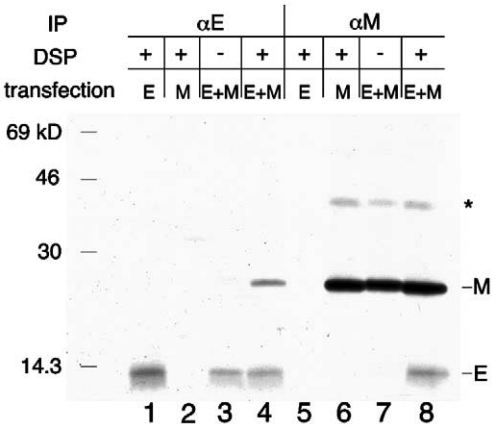

Fig. 2. IBV E and M interact in transfected OST7-1 cells. OST7-1 cells expressing E and M proteins alone or together were labeled with [^{35}S]methionine-cysteine, treated with DSP as indicated, lysed, and immunoprecipitated with anti-E or anti-M antibodies as described under Materials and methods. All immunoprecipitates in this and the following figures were deglycosylated by treating with *N*-glycanase to collapse the M protein to a single band. The immunoprecipitates were analyzed by SDS–17.5% PAGE in the presence of βME, and fluorography. The asterisk indicates a band that corresponds to M protein dimers. These data are representative of at least three independent experiments.

and Inglis, 1991), which is presumably determined by the stoichiometry of envelope protein interactions. We conclude that the IBV E and M proteins interact in infected cells.

IBV E and M proteins directly interact when expressed in the absence of a virus infection

IBV-infected cells contain other viral proteins which might be required for interaction of E and M. To determine if the IBV E and M proteins could interact directly, we coexpressed them in OST7-1 cells. We used indirect immunofluorescence to verify coexpression and correct intracellular localization of the two proteins (Fig. 3A, panels a–c). As expected, the IBV E and M proteins colocalized in a compact perinuclear region characteristic of the Golgi complex in this cell type, as seen previously in BHK-21 cells (Corse and Machamer, 2000). When we treated OST7-1 cells coexpressing IBV E and M with DSP and analyzed anti-E and anti-M immunoprecipitates as described above, we found that M protein was present in the anti-E immunoprecipitate (Fig. 2, lane 4) and that E protein was present in the anti-M immunoprecipitate (Fig. 2, lane 8), suggesting that the two proteins directly interact in transfected cells. Detection of the interaction required crosslinking (compare lanes 3 and 7 to lanes 4 and 8) and antisera specific for E or M. Even though less E was expressed in transfected cells (Fig. 2) compared to IBV-infected cells (Fig. 1B), the ratio of E:M crosslinks (as seen in the relative amounts of E and M in the anti-M and anti-E immunoprecipitations, respectively) was similar, suggesting that there is a precise stoichiometry of interaction.

To investigate which domains of the E and M proteins interact, we made use of a panel of mutant E and M proteins that were generated to study the Golgi targeting signals present in the two proteins (Corse and Machamer, 2002; Machamer and Rose, 1987). Although many mutant E and M proteins have been generated, in this study, we used only those that are properly targeted to the Golgi region. Since these mutant proteins had previously been localized in BHK-21 or COS-7 cells, we first confirmed that they were properly targeted in OST-7 cells. Cells coexpressing wild-type M protein and E mutants were analyzed by indirect immunofluorescence microscopy (Fig. 3A). EG3 (panels d–f) contains the transmembrane domain from the plasma membrane protein vesicular stomatitis virus (VSV) G; CTE (panels g–i) is an N-terminal truncation of IBV E consisting only of its cytoplasmic tail, and GEt (panels j–l) is a chimeric protein containing the lumenal and transmembrane domains of VSV G and the cytoplasmic tail of IBV E. In all cases, the E mutant proteins were correctly localized to the Golgi region of OST7-1 cells (including the partial transmembrane replacement mutants EG1 and EG2, not shown), consistent with our previous studies in BHK-21 cells (Corse and Machamer, 2002). Fig. 3B shows cells that are coexpressing wild-type E protein and the M protein deletion mutants MctΔ1 (panels a–c), which is missing cytoplasmic tail amino acid residues 103–203, MctΔ2 (panels d–f), which is missing cytoplasmic tail residues 119–203, MctΔ3 (panels g–i), which is missing cytoplasmic tail residues 103–118, or MΔm2,3 (panels j–l), which is missing the second and third transmembrane domains (amino acid residues 43–101). The M mutants, especially MctΔ3 (Fig. 3B, panel h) and MΔm2,3 (Fig. 3B, panel k), were incompletely localized to the Golgi region, since some ER staining was observed. However, they all reached the Golgi to some extent, as indicated by the juxtanuclear spot.

The cytoplasmic tail of IBV E is sufficient for its interaction with IBV M

We asked whether the E transmembrane replacement mutants EG1, EG2, and EG3 (in which the first third, the first two-thirds, or the entire E transmembrane domain, respectively, were replaced with the corresponding regions of the VSV G transmembrane domain) (Corse and Machamer, 2002) could be crosslinked to wild-type M protein. The appropriate proteins were coexpressed and immunoprecipitated with anti-E or anti-M antibodies after treating the cells with DSP as described above (Fig. 4A). All three E transmembrane replacement mutants were crosslinked to M protein, suggesting that the E transmembrane domain is not required for E and M interaction. However, there was less M in the anti-E immunoprecipitation of EG3 (Fig. 4A, lane 4), suggesting that the interaction of M with this mutant could be decreased. Perhaps the E and M transmembrane domains interact, or the conformation of the cytoplasmic

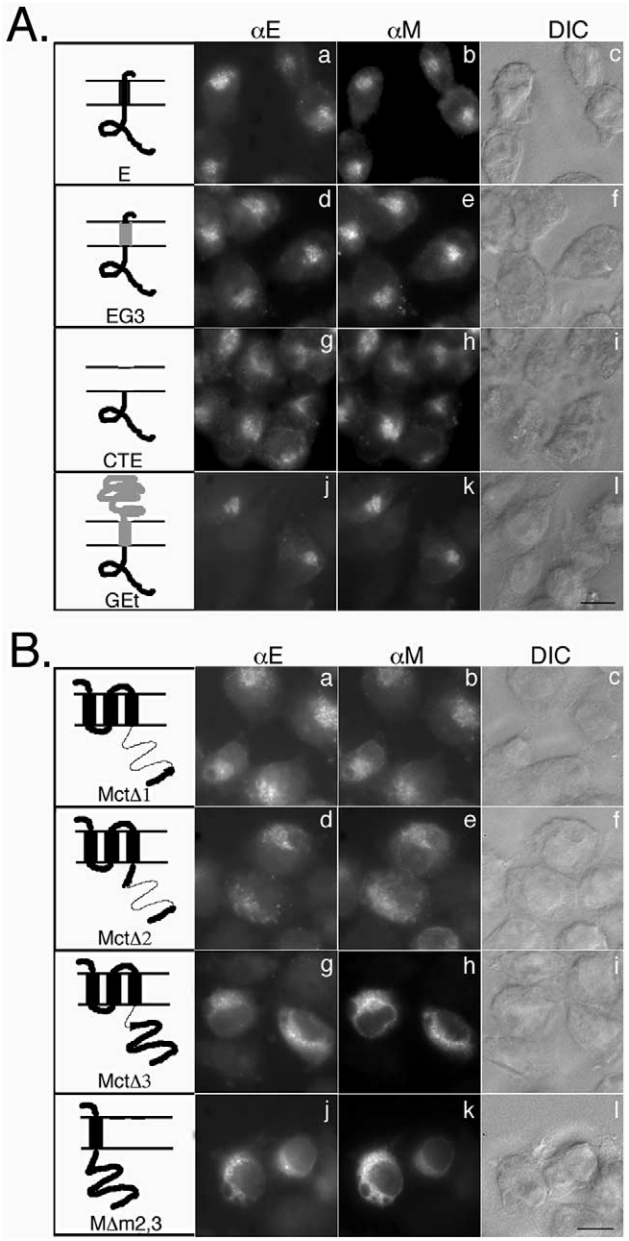

Fig. 3. The wild-type and mutant versions of IBV E and IBV M proteins used in this study are localized to the Golgi region of transfected OST7-1 cells. (A) OST7-1 cells expressing wild-type IBV E and M proteins (a–c), EG3 and wild-type M protein (d–f), CTE and wild-type M protein (g–i), or GEt and wild-type M protein (j–l) were fixed for immunofluorescence and double labeled with rat anti-E antibody (a, d, g, and j) and rabbit anti-M antibody (b, e, h, and k). Secondary antibodies were fluorescein-conjugated goat anti-rat IgG and Texas red conjugated donkey anti-rabbit IgG. The third image in each row (c, f, i, and l) is a DIC image of the labeled cells. In the diagrams of the E mutant and chimeric proteins, IBV E sequence is shown in black and VSV G sequence is shown in gray. Bar, 10 μm. (B) OST7-1 cells expressing wild-type E protein and MctΔ1 (a–c), MctΔ2 (d–f), MctΔ3 (g–i), or MΔm2,3 (j–l) were fixed for immunofluorescence and double labeled with rat anti-E antibody (a, d, g, and j) and rabbit anti-M antibody (b, e, h, and k). Secondary antibodies were fluorescein-conjugated goat anti-rat IgG and Texas red conjugated donkey anti-rabbit IgG. The third image in each row (c, f, i, and l) is a DIC image of the labeled cells. In the diagrams of the deletion mutant M proteins, the thin lines indicate deleted sequence. Bar, 10 μm.

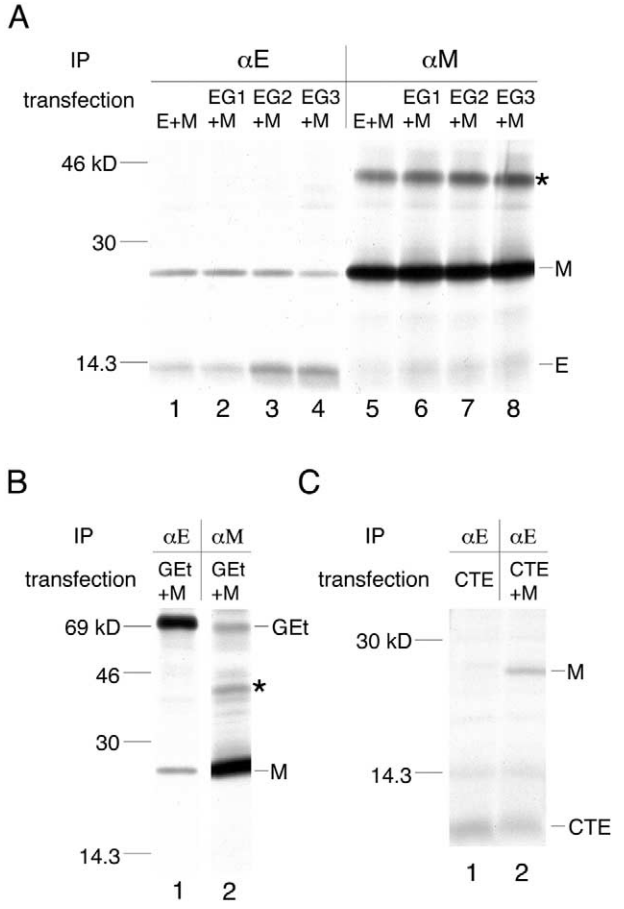

Fig. 4. The cytoplasmic tail of IBV E is sufficient for interaction with IBV M. (A) OST7-1 cells expressing wild-type M protein and wild-type E protein or the E transmembrane replacement mutant proteins EG1, EG2, or EG3 were labeled with [^{35}S]methionine-cysteine, treated with DSP, lysed, and immunoprecipitated with anti-E or anti-M antibodies as described under Materials and methods. The immunoprecipitates were analyzed by SDS–17.5% PAGE in the presence of βME, and fluorography. The asterisk indicates a band that corresponds to M protein dimers. (B) OST7-1 cells coexpressing the GEt chimera and wild-type M protein were labeled with [^{35}S]methionine-cysteine, treated with DSP, lysed, and immunoprecipitated with anti-E or anti-M antibodies as described under Materials and methods. The immunoprecipitates were analyzed by SDS–15% PAGE in the presence of βME, and fluorography. The asterisk indicates a band that corresponds to M protein dimers. (C) OST7-1 expressing CTE protein alone or with M protein were labeled with [^{35}S]methionine-cysteine, treated with DSP, lysed, and immunoprecipitated with anti-E antibodies as described under Materials and methods. The immunoprecipitates were analyzed by SDS–17.5% PAGE in the presence of βME, and fluorography. These data are representative of at least three independent experiments.

tail of E is altered when the complete transmembrane domain is replaced (see below).

To evaluate the role of the E cytoplasmic tail in interaction with M, we tested whether the chimeric protein GEt (which consists of the cytoplasmic tail of IBV E and the transmembrane and lumenal domains of VSV G; see Fig. 3A) could be crosslinked to M (Fig. 4B). As shown in Fig. 4B, lane 1, M was found in the immunoprecipitation with anti-E antibody, which recognizes the last 14 amino acids of

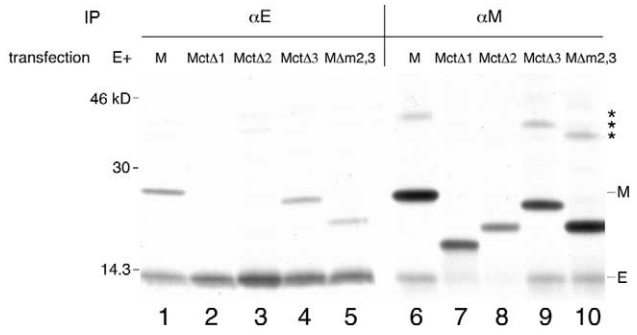

Fig. 5. A region of the IBV M cytoplasmic tail is required for crosslinking to IBV E. OST7-1 cells expressing wild-type E protein and wild-type M protein or the M deletion mutant proteins MctΔ1, MctΔ2, MctΔ3, or MΔm2,3 were labeled with [^{35}S]methionine-cysteine, treated with DSP, lysed, and immunoprecipitated with anti-E or anti-M antibodies as described under Materials and methods. The immunoprecipitates were analyzed by SDS–17.5% PAGE in the presence of βME, and fluorography. The asterisks indicate bands that correspond to M, MctΔ3, or MΔm2,3 protein dimers. These data are representative of at least three independent experiments.

the E cytoplasmic tail and thus the GEt chimera. The reciprocal immunoprecipitation with anti-M antibody contained GEt protein (lane 3). We conclude that the cytoplasmic tail of IBV E protein is sufficient for interaction with M protein. Indeed, the N-terminal truncation mutant CTE, which consists only of the cytoplasmic tail of IBV E (Corse and Machamer, 2002), was coprecipitated with M after crosslinking (Fig. 4C, lane 2). We previously found that partial or complete removal of a 50 amino acid region within the 80 amino acid E cytoplasmic tail resulted in transport of the GEt chimera to the cell surface (Corse and Machamer, 2002). Therefore, we did not attempt to find a specific region within the IBV E cytoplasmic tail that interacts with IBV M, because colocalization of the IBV E and M proteins is likely to be required for their interaction.

The IBV M cytoplasmic tail is required for crosslinking to IBV E

To determine which regions of the IBV M protein were involved in interaction with IBV E, we tested how well the M deletion mutants MctΔ1, MctΔ2, MctΔ3, and MΔm2,3 could be crosslinked to wild-type E protein compared to wild-type M protein (Fig. 5). MΔm2,3 is missing the second and third transmembrane domains of IBV M; since it was crosslinked to E protein as well as wild-type M (lanes 5 and 10), we conclude that these membrane- spanning regions are not involved in interactions with E. A large portion of the M cytoplasmic tail is deleted in MctΔ1 (see Fig. 3B), and this protein was not crosslinked efficiently to E, compared to wild-type M protein (Fig. 5, lanes 2 and 7), although a small amount of E protein is visible in the MctΔ1 immunoprecipitation (Fig. 5, lane 7). This result indicates that the M cytoplasmic tail is involved in interaction with E. The portion of the M cytoplasmic tail removed by the MctΔ1 deletion is split into parts by the MctΔ2 and MctΔ3 deletions. Note that the MctΔ1 and MctΔ2 mutants are not radiolabeled as efficiently as wild-type M and the MctΔ3 and MΔm2,3 mutants (compare lanes 7 and 8 with lane 6) because they have fewer methionines and cysteines due to their deletions, which could explain why a reciprocal amount of MctΔ1 is not seen in the anti-E immunoprecipitation (Fig. 5, lane 2). MctΔ3, which is missing amino acids 103–118 of the M cytoplasmic tail, was crosslinked to E (Fig. 5, lanes 4 and 9), while MctΔ2, which is missing amino acids 119–203 of the M cytoplasmic tail (see Fig. 2B), was not (Fig. 5, lanes 3 and 8). This indicates that the amino acids removed by the MctΔ2 deletion (119–203) are required for crosslinking of the IBV M protein to the IBV E protein.

The transmembrane domain of IBV E is not required for VLP formation

The E and M proteins of several coronaviruses are released from cotransfected cells in membrane-bound particles that are morphologically similar to virions (VLPs), suggesting that interactions between these proteins are an integral part of coronavirus assembly (Baudoux et al., 1998; Corse and Machamer, 2000; Godeke et al., 2000; Vennema et al., 1996). We initially attempted to study VLPs formed in BHK cells from IBV E and M proteins expressed by coinfection with recombinant vaccinia viruses encoding each protein. However, we found that VLP formation was extremely inefficient under these conditions and estimated that only 0.01% of the cellular E and M proteins were released into the supernatant as VLPs (Corse and Machamer, 2000). Since we were interested in using VLP formation to delineate portions of the IBV E and M proteins that are important in virus assembly, we employed the expression system used by Rottier and colleagues in their initial description of MHV VLPs (Vennema et al., 1996). These authors infected OST7-1 cells (Elroy-Stein and Moss, 1990), which are osteosarcoma cells that stably express phage T7 RNA polymerase, with a vaccinia virus encoding T7 polymerase (vTF7-3) (Fuerst et al., 1986) to provide higher levels of T7 RNA polymerase. They then transfected the cells with plasmids encoding MHV E and M behind the T7 promoter. When we expressed the IBV E and M proteins this way, we found that VLPs were formed efficiently (Fig. 6, lanes 3 and 14). The supernatant side of the gel (lanes 12–22) shown in this figure was exposed 20 times longer than the cell side to allow the visualization of E and E transmembrane mutant proteins (lanes 1–11). We have consistently observed at least 10%, and frequently more, of the cellular M protein being released into the supernatant during the 3 h chase (data not shown). This level of VLP release was dependent on E protein, since less than 1% of the cellular M protein was found in the supernatant in the absence of E. E protein was not visualized in the supernatants when expressed alone (Fig. 6, lane 12). We believe that a small amount of E is released into the supernatant

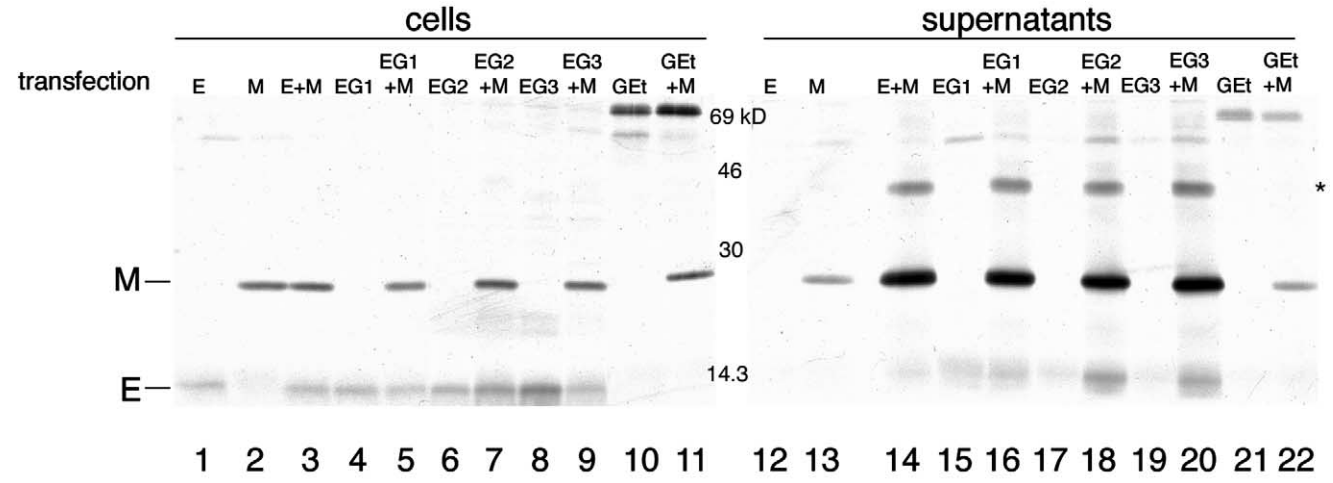

Fig. 6. Complete replacement of the E transmembrane domain does not affect VLP formation. OST7-1 cells expressing the indicated proteins were labeled with [^{35}S]methionine-cysteine for 1 h and chased for 3 h, and the supernatants and cells were harvested and immunoprecipitated with anti-E and anti-M antibodies as described under Materials and methods. The immunoprecipitates were analyzed by SDS–17.5% PAGE and fluorography. The supernatant samples (lanes 12–22) were exposed to film 20 times longer than the cell samples (lanes 1–11) to allow the visualization of EG2 and EG3 proteins in lanes 18 and 20, respectively. The asterisk indicates a band that corresponds to dimers of M protein. These data are representative of at least three independent experiments.

when it is expressed alone, and that it is simply not visualized unless a large amount of supernatant is loaded on the gel, as in our previous experiments (Corse and Machamer, 2000). Our results differ from the data of Makino and colleagues, who observed a substantial amount of MHV E being released into the supernatant when expressed by itself (Maeda et al., 1999); this discrepancy could be explained by the different expression system used to produce the E protein in their study. We favor the hypothesis that VLP formation involves a lattice of M protein within the membrane with curvature induced by small amounts of the E protein (De Haan et al., 2000) (see Discussion). This would account for the small amount of IBV E protein relative to IBV M protein that is found in VLPs.

We found that the partial or complete replacement of the IBV E transmembrane domain (mutants EG1, EG2, and EG3) had no effect on E's ability to induce VLPs as measured by the amount of IBV M protein released into the supernatant (Fig. 6, compare the M protein bands in lanes 14, 16, 18, and 20). We did notice that more EG2 and EG3 proteins were incorporated into VLPs compared to wild-type E and EG1 proteins (Fig. 6, compare the E protein bands in lanes 18 and 20 with those in lanes 14 and 16). It is possible that conformational changes induced by replacement of the transmembrane domain facilitates increased incorporation of these mutants into VLPs. The EG2 and EG3 mutants did not induce VLPs more efficiently than wild-type E, because an increased amount of M protein was not released into the supernatant.

We examined the ability of the E cytoplasmic tail to induce VLPs by using the chimeric protein GEt. When expressed by itself, we observed that a negligible amount of this protein was released into the supernatant (Fig. 6, lane 21; recall that the supernatant side of the gel was exposed 20 times longer than the cell side) and that expression of GEt with IBV M did not increase the amount of M that was released when M was expressed alone (Fig. 6, lanes 22 and 13). We conclude that the GEt chimera does not induce VLPs. Since both the EG3 and the GEt chimeras contain the transmembrane domain of VSV G and the cytoplasmic tail of IBV E, it seems likely that the VSV G lumenal domain is incompatible with VLP formation, either because it is too large or because it cannot be incorporated into the M protein lattice for some other reason (see Discussion). Thus, it is difficult to predict if the E cytoplasmic tail alone is capable of inducing VLPs. We also did not observe VLP formation with the IBV E N-terminal truncation mutant CTE, which consists only of the E cytoplasmic tail (data not shown). However, this result is inconclusive since the CTE protein is less stable than wild-type E protein and thus accumulates to significantly lower levels (Corse and Machamer, 2002).

VLP formation with mutant IBV M proteins does not correlate with crosslinking to IBV E

We evaluated the incorporation of the IBV M deletion mutants MctΔ1, MctΔ2, MctΔ3, and MΔm2,3 into VLPs. As shown in Fig. 7, none of the deletion mutants were able to support VLP formation at a detectable level, regardless of whether they could be crosslinked to IBV E. The MctΔ1 and MctΔ2 mutants are not radiolabeled as efficiently as wild-type M and the MctΔ3 and MΔm2,3 mutants (compare lanes 5,6,7, and 8 with lanes 2 and 3) because they have fewer methionines and cysteines due to their deletions. However, we would still expect to see a detectable signal in the supernatants after a long exposure if these mutants supported VLP formation at a level comparable to wild-type

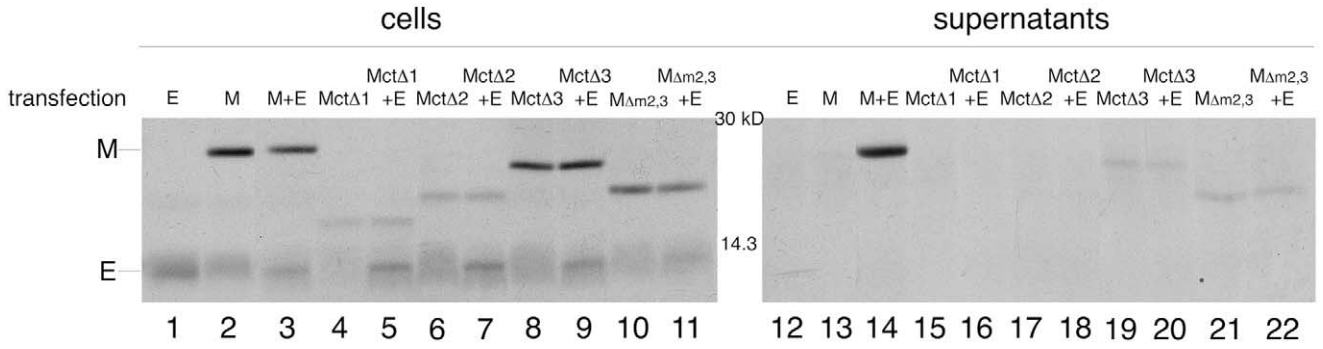

Fig. 7. Cytoplasmic and transmembrane region deletion mutants of IBV M do not support VLP formation. OST7-1 cells expressing the indicated proteins were labeled with with [^{35}S]methionine-cysteine for 1 h and chased for 3 h, and the supernatants and cells were harvested and immunoprecipitated with anti-E and anti-M antibodies as described under Materials and methods. The immunoprecipitates were analyzed by SDS–17.5% PAGE and fluorography. The supernatant samples (lanes 12–22) were exposed to film 13 times longer than the cell samples (lanes 1–11). The MctΔ1 and MctΔ2 mutants are not radiolabeled as efficiently as wild-type M and the MctΔ3 and MΔm2,3 mutants because they have fewer methionines and cysteines due to their deletions. These data are representative of at least three independent experiments.

M. Since we have never seen such a signal, we conclude that these mutants do not support VLP formation.

These results indicate that both the cytoplasmic tail and the transmembrane regions of IBV M are involved in VLP formation, which is consistent with the results of Rottier and colleagues, who found that mutations in all domains of the MHV M protein abrogated VLP formation (De Haan et al., 1998). These results suggest that a direct interaction between IBV E and M proteins is not sufficient for VLP formation and that this process may depend on how the two proteins interact with the membrane bilayer, both separately and together.

Discussion

We have demonstrated an interaction between the IBV E and M proteins using both in vivo chemical crosslinking and VLP formation as assays. Using IBV E and M protein mutants that were generated in the course of Golgi targeting studies, we examined the domains in the IBV E and M proteins that are involved in their interaction. We found that the cytoplasmic tails of both proteins mediate their interaction, as measured by crosslinking. Interestingly, however, we observed that reciprocal crosslinking of IBV E and M protein mutants did not correlate with VLP formation, suggesting that interaction between IBV E and M is not sufficient for VLP formation. Here we compare our results to those reported by other groups and discuss the implications of our findings for coronavirus assembly.

Cytoplasmic tail of IBV E and its interaction with IBV M

Lim and Liu previously used a coimmunoprecipitation assay to detect IBV E and M protein interactions (Lim and Liu, 2001). They also concluded that the cytoplasmic tail of IBV E is important for interaction with IBV M, since deletion of a 20 amino acid region within the E cytoplasmic tail (amino acids 37–57) prevented coimmunoprecipitation of the E and M proteins and VLP formation. As mentioned above, we did not attempt to find a region within the E tail that mediates its interaction with IBV M, because we previously found that partial or complete replacement of a 50 amino acid region in the IBV E tail results in transport of a reporter chimera from the Golgi complex to the cell surface, which indicates that the cytoplasmic tail of E contains Golgi targeting information (Corse and Machamer, 2002). Our subcellular localization results differ from those of Lim and Liu, who reported that IBV E is localized to the endoplasmic reticulum of transfected cells (Lim and Liu, 2001), possibly because they examined cells overexpressing epitope-tagged IBV E protein.

Coronavirus M protein and VLP formation

The M protein is by far the most abundant envelope protein of coronaviruses and has been estimated to account for ~40% of the mass of IBV and MHV particles (Stern et al., 1982; Sturman et al., 1980). Thus the physical nature of the coronavirus envelope must be largely determined by the characteristics of the M protein. Interestingly, however, the M protein cannot drive coronavirus budding by itself, but displays a strict requirement for a small amount of E protein for VLP formation (Baudoux et al., 1998; Corse and Machamer, 2000; Godeke et al., 2000; Vennema et al., 1996). We have observed this low E protein:M protein ratio in IBV VLPs (Fig. 6, lane 14); measurements of the amount of E and M proteins in IBV virions also reveal a relatively low amount of E protein (Liu and Inglis, 1991). We favor the hypothesis that VLP formation involves a specific membrane curvature that is induced by the proper ratio of M and E proteins. The mechanism by which a small amount of E protein interacts with a large amount of M protein to induce invagination and pinching of the membrane to form VLPs

remains unclear, but its elucidation is likely to be essential for a complete understanding of coronavirus assembly. Several studies have addressed the question of how the coronavirus E and M proteins interact in VLP formation.

Rottier and colleagues (De Haan et al., 1998) studied the primary sequence requirements for incorporation of the MHV M protein into VLPs. They found that all regions of MHV M seem to be important for VLP formation, since mutations in the short lumenal domain, the transmembrane region, and the cytoplasmic tail all impaired VLP formation to some extent. These results are consistent with our observation that deletions in both the cytoplasmic and the transmembrane domains of IBV M prevent VLP formation. Interestingly, the extreme C-terminus of the cytoplasmic tail MHV M was found to be especially important, since deletion of only the C-terminal threonine residue prevented VLP formation (De Haan et al., 1998). We were unable to examine the role of the extreme C-terminus of the IBV M protein in VLP formation because our antibody to IBV M recognizes this sequence.

Laude and colleagues (Baudoux et al., 1998) showed that coexpression of the E and M proteins of transmissible gastroenteritis virus (TGEV) and of bovine coronavirus (BCV) resulted in VLP production. In this study VLPs were also produced with a BCV- TGEV chimeric M protein. Interestingly, the chimeric M protein was able to form VLPs with TGEV E, BCV E, and BCV-TGEV chimeric E proteins. Since TGEV and BCV are in different coronavirus groups based on serological and genomic sequence relationships, this suggests that VLP formation does not depend on interactions between E and M proteins that are based on strict sequence requirements. Well-conserved three- dimensional characteristics of the E and M proteins may be instrumental in VLP formation.

Crosslinking of IBV E and M protein mutants is not sufficient for VLP formation

Our results suggest that VLP formation involves more than an interaction between E and M proteins, since M protein mutants that could be crosslinked to E protein (MctΔ3 and MΔm2,3; see Fig. 5) are not incorporated into virus-like particles. It is possible that VLP formation requires interactions between M proteins, as proposed by Rottier and colleagues (De Haan et al., 2000). These workers demonstrated homotypic interactions among MHV M protein molecules by coimmunoprecipitation and incorporation of VLP assembly-incompetent MHV M mutants into VLPs via their interaction with assembly-competent MHV M proteins. These authors hypothesize that the VLP (and virion) envelope mainly consists of an M protein lattice, with a few E proteins interspersed within this lattice. Although we have not examined whether homotypic interactions between IBV M proteins exist, we think it possible that such interactions may be important in IBV VLP assembly. We did observe a small amount of SDS-resistant IBV M protein dimers in our anti-M immunoprecipitations (indicated by asterisks in Figs. 2, 4, 5, and 6), although we have no direct evidence that these dimers are physiologically relevant.

We also showed that the GEt chimera could be crosslinked to IBV M protein (Fig. 4B), but did not induce VLP formation (Fig. 6). Since the GEt chimera contains the same transmembrane domain and cytoplasmic tail as the transmembrane replacement mutant EG3, which was able to induce VLP formation as well as wild-type E protein (Fig. 6), a likely explanation is that the VSV G ectodomain prevents induction of VLPs. One possibility is that this large ectodomain does not fit well into the lattice of M protein in the membrane. A similar observation was reported by Rottier and colleagues (De Haan et al., 2000), who showed that foreign proteins such as wild-type VSV G protein, equine arteritis virus M protein, and CD8 were effectively excluded from MHV VLPs. Likewise, it is possible that the M deletion mutants we tested in the VLP assay are not in the right conformation to fit into such a lattice of M protein, and thus, do not support VLP formation.

The role of the IBV E cytoplasmic tail in interaction with both IBV M and Golgi targeting

As mentioned above, we have previously shown that the cytoplasmic tail of the IBV E protein is sufficient to localize it to the Golgi complex and to mediate its redistribution with the Golgi scaffold proteins GM130 and p115 during brefeldin-A treatment (Corse and Machamer, 2002). Since these and other Golgi scaffold proteins are known to be part of a complex which is thought to mediate vesicle tethering during intra-Golgi transport (Barr et al., 1998; Seemann et al., 2000a,b), this led us to hypothesize that the IBV E protein may be targeted to the Golgi apparatus via a direct interaction with one or more Golgi scaffold proteins. Furthermore, interaction of IBV E with the Golgi scaffold could result in modulation of vesicular traffic, which might be advantageous for collecting coronavirus envelope proteins in a specific Golgi compartment for assembly (Corse and Machamer, 2002).

Since we have shown here that the cytoplasmic tail of IBV E is also important for interactions with IBV M, this raises the question of whether the E cytoplasmic tail can interact with M and the Golgi scaffold simultaneously. If not, then it is possible that two functional pools of IBV E protein exist in an infected cell. One pool could interact with IBV M and the membrane at the assembly site to induce virus budding, while the other could associate with the Golgi scaffold to influence vesicular traffic through the Golgi complex. The latter interaction might aid in collecting viral membrane proteins for assembly at Golgi membranes. Since the small amount of IBV E protein found in virions (Liu and Inglis, 1991) and VLPs (shown here) suggests that not much E protein is required to induce virus budding, maybe a second function of E protein, such as modulation of Golgi transport, accounts for the apparent excess of IBV E protein in infected cells (Corse and Machamer, 2000).

Materials and methods

Cells and viruses

OST7-1 cells (Elroy-Stein and Moss, 1990) and Vero cells were maintained in Dulbecco's modified Eagle's medium (DMEM) containing 10% fetal calf serum (FCS) and antibiotics. The adaptation of IBV (Beaudette strain) to Vero cells has been described (Machamer and Rose, 1987). The recombinant vaccinia viruses encoding phage T7 polymerase (vTF7-3), IBV M (vvIBVM), and wild-type and mutant versions of IBV E (vvIBVE, vvEG3, vvCTE) have been described (Corse and Machamer, 2000, 2002; Fuerst et al., 1986; Machamer and Rose, 1987). Growth and titering of recombinant vaccinia viruses were done as described (Weisz and Machamer, 1994).

Expression plasmids

The pBS/IBV E, pBS/EG1, pBS/EG2, pBS/EG3, pBS/GEt, pAR/M and pAR/MΔm2,3 plasmids have been described (Corse and Machamer, 2000, 2002; Machamer and Rose, 1987). IBV M was subcloned into the *Bam*HI site of pT7/T3-18 (BRL) to create pT7/M. The M cytoplasmic tail deletion mutant plasmids pAR/MctΔ1, pAR/MctΔ2, and pAR/MctΔ3 were constructed by oligonucleotide-directed mutagenesis as described (Machamer and Rose, 1987). MctΔ1 is missing amino acids 103–203, MctΔ2 is missing amino acids 119–203, and MctΔ3 is missing amino acids 103–118. All three of these cytoplasmic tail deletion mutants contain the IBV M C-terminal 22 amino acids that are recognized by the polyclonal anti-M antibody (see Fig. 3B). pAR/E and pAR/CTE were made by PCR addition of *Bam*HI sites at both ends of the E and CTE inserts. pBS/IBV E and pBS/CTE (Corse and Machamer, 2002), respectively, were used as templates for PCR. The *Bam*HI-digested PCR products were cloned into the *Bam*HI site of pAR2529, and subclones were screened for correct orientation by indirect immunofluorescence. The pT7/McΔ1, pT7/MctΔ2, and pT7/MctΔ3 plasmids used in VLP experiments were made by PCR addition of *Eco*RI and *Xba*I restriction sites, with the corresponding AR plasmids as templates. The T7/MΔm2,3 plasmid used in VLP experiments was made by subcloning the pAR/MΔm2,3 *Bam*HI fragment into the the *Bam*HI site of pT7/T3-18.

Antibodies

The polyclonal anti-M antibody and its affinity purification for use in immunofluorescence has been previously described (Machamer and Rose, 1987). The rat and rabbit polyclonal antibodies to the C-terminal 14 amino acids of IBV E have been reported (Corse and Machamer, 2000). The rabbit anti-VSV polyclonal antibody used to immunoprecipitate radiolabeled G and GEt proteins has been described (Weisz et al., 1993). Texas red conjugated donkey anti-rabbit immunoglobulin G (IgG) and fluorescein-conjugated goat anti-rat IgG were from Jackson ImmunoResearch Laboratories, Inc. (West Grove, PA).

Immunofluorescence microscopy

Vero cells were plated in 35-mm dishes 1 day before being infected with IBV (passage 12), as previously described (Machamer and Rose, 1987). The cells were fixed in 3% paraformaldehyde in phosphate-buffered saline (PBS) for 20 min at room temperature, permeabilized with 0.5% Triton X-100, and stained as previously described (Swift and Machamer, 1991) with rat anti-E antibody and rabbit anti-M antibody. OST7-1 cells were plated on cover slips in 35-mm dishes 2 days before infection with vTF7-3, vvIBVE, vvEG3, or vvCTE at a multiplicity of infection of 20. Adsorption was for 1 h at 37°C, and cells infected with vTF7-3 were transfected with 5 μg of each expression plasmid using 20 μl of Lipofectin (Invitrogen, Carlsbad, CA) as directed by the manufacturer. At 3.5 to 4 h postinfection the cells were fixed and stained as described above.

Chemical crosslinking

OST7-1 cells were plated in 35-mm dishes 2 days before being infected with vTF7-3 and transfected with the appropriate constructs as described above. In samples transfected with only a plasmid encoding IBV E or IBV M alone, an equal amount of empty vector plasmid was added so that an equal amount of plasmid DNA was added to all samples. At 4 h postinfection, the cells were labeled with 100 μCi of ^{35}S-Promix (Amersham Pharmacia Biotech, Piscataway, NJ) in 0.5 ml methionine- and cysteine-free medium for 1 to 1.5 h at 37°C. Vero cells were plated in a 10-cm dish 1 day before being infected with IBV and labeled at 45 h postinfection for 1 h at 37°C with 500 μCi of ^{35}S-Promix. After being rinsed twice in room temperature PBS, cells were scraped into PBS, transferred to microfuge tubes, and the thiol-cleavable crosslinker DSP (Pierce, Rockford, IL) was added to 1 mM after being prepared just before use as a 20 mM stock solution in DMSO. For mock DSP treatments an equivalent amount of DMSO was added. The cells were incubated with DSP for 10 min at room temperature, and the DSP was quenched by adding glycine to 40 mM. The cells were lysed in detergent solution [62.5 mM EDTA, 50 mM Tris (pH 8), 0.4% deoxycholate, 1% NP-40] containing protease inhibitors, and the postnuclear supernatants were immunoprecipitated with the appropriate antibodies in the presence of 0.2% SDS as described (Machamer and Rose, 1987). Treatment of immunoprecipitates with *N*-glycanase was as previously described (Machamer et al., 1990). The samples were subjected to SDS–PAGE in the presence of β- mercaptoethanol (except for the indicated samples in Fig. 1B) and the labeled proteins were visualized by fluorography.

Virus-like particles

Appropriate constructs were expressed in OST7-1 cells by infection with vTF7-3 and transfection as described above. At 3 h postinfection the cells were shifted from 37 to 32°C for 1 h and then radiolabeled at 32°C with ^{35}S-Promix for 1 to 1.5 h as described above. After labeling the cells were chased in 1 ml of growth medium for 3 h at 32°C. The medium was microcentrifuged at 14,000 rpm for 20 min at 4°C to remove cellular debris, and the supernatants were immunoprecipitated with rat anti-E and rabbit anti-M antibodies in the presence of 1% Triton X-100 and 0.2% SDS. The cells were harvested by rinsing in PBS and lysing in detergent solution. The postnuclear supernatants were immunoprecipitated with anti-E and anti-M antibodies in the presence of 0.2% SDS. The immunoprecipitates were treated with *N*-glycanase as described (Machamer et al., 1990).

Acknowledgments

This work was supported by National Institutes of Health Grants GM42522 and GM64647. We thank the members of the Machamer lab for critical reading of the manuscript.

References

Barr, F.A., Nakamura, N., Warren, G., 1998. Mapping the interaction between GRASP65 and GM130, components of a protein complex involved in the stacking of Golgi cisternae. EMBO J. 17, 3258–3268.

Baudoux, P., Carrat, C., Besnardeau, L., Charley, B., Laude, H., 1998. Coronavirus pseudoparticles formed with recombinant M and E proteins induce alpha interferon synthesis by leukocytes. J. Virol. 72, 8636–8643.

Corse, E., Machamer, C.E., 2000. Infectious bronchitis virus E protein is targeted to the Golgi complex and directs release of virus-like particles. J. Virol. 74, 4319–4326.

Corse, E., Machamer, C.E., 2001. Infectious bronchitis virus envelope protein targeting: implications for virus assembly. Adv Exp. Med. Biol. 494, 571–576.

Corse, E., Machamer, C.E., 2002. The cytoplasmic tail of infectious bronchitis virus E protein directs Golgi targeting. J. Virol. 76, 1273–1284.

De Haan, C.A., Kuo, L., Masters, P.S., Vennema, H., Rottier, P.J., 1998. Coronavirus particle assembly: primary structure requirements of the membrane protein. J. Virol. 72, 6838–6850.

De Haan, C.A., Vennema, H., Rottier, P.J., 2000. Assembly of the coronavirus envelope: homotypic interactions between the M proteins. J. Virol. 74, 4967–4978.

Dubois-Dalcq, M., Holmes, K.V., Rentier, B. 1984. Assembly of Enveloped RNA Viruses. Kingsbury, D.W. (Ed.) Springer-Verlag, Wien New York.

Elroy-Stein, O., Moss, B., 1990. Cytoplasmic expression system based on constitutive synthesis of bacteriophage T7 RNA polymerase in mammalian cells. Proc. Natl. Acad. Sci. USA 87, 6743–6747.

Fischer, F., Stegen, C.F., Masters, P.S., Samsonoff, W.A., 1998. Analysis of constructed E gene mutants of mouse hepatitis virus confirms a pivotal role for E protein in coronavirus assembly. J. Virol. 72, 7885–7894.

Fuerst, T.R., Giles, E.G., Studier, F.W., Moss, B., 1986. Eukaryotic transient expression system based on recombinant vaccinia virus that synthesizes bacteriophage T7 RNA polymerase. Proc. Nat. Acad Sci. 83, 8122–8126.

Garoff, H., Hewson, R., Opstelten, D.J., 1998. Virus maturation by budding. Microbiol. Mol. Biol. Rev. 62, 1171–1190.

Godeke, G.J., De Haan, C.A., Rossen, J.W., Vennema, H., Rottier, P.J., 2000. Assembly of spikes into coronavirus particles is mediated by the carboxy-terminal domain of the spike protein. J. Virol. 74, 1566–1571.

Griffiths, G., Rottier, P., 1992. Cell biology of viruses that assemble along the biosynthetic pathway. Semin. Cell. Biol. 3, 367–381.

Hung, T., Chou, Z.Y., Zhao, T.X., Xia, S.M., Hang, C.S., 1985. Morphology and morphogenesis of viruses of hemorrhagic fever with renal syndrome (HFRS). I. Some peculiar aspects of the morphogenesis of various strains of HFRS virus. Intervirology 23, 97–108.

Klumperman, J., Locker, J.K., Meijer, A., Horzinek, M.C., Geuze, H.J., Rottier, P.J., 1994. Coronavirus M proteins accumulate in the Golgi complex beyond the site of virion budding. J. Virol. 68, 6523–6534.

Lim, K.P., Liu, D.X., 2001. The missing link in coronavirus assembly. Retention of the avian coronavirus infectious bronchitis virus envelope protein in the pre-Golgi compartments and physical interaction between the envelope and membrane proteins. J. Biol. Chem. 276, 17515–17523.

Liu, D.X., Inglis, S.C., 1991. Association of the infectious bronchitis virus 3c protein with the virion envelope. Virology 185, 911–917.

Machamer, C.E., Grim, M.G., Esquela, A., Chung, S.W., Rolls, M., Ryan, K., Swift, A.M., 1993. Retention of a cis Golgi protein requires polar residues on one face of a predicted alpha-helix in the transmembrane domain. Mol. Biol. Cell 4, 695–704.

Machamer, C.E., Mentone, S.A., Rose, J.K., Farquhar, M.G., 1990. The E1 glycoprotein of an avian coronavirus is targeted to the cis Golgi complex. Proc. Natl. Acad. Sci. USA 87, 6944–6948.

Machamer, C.E., Rose, J.K., 1987. A specific transmembrane domain of a coronavirus E1 glycoprotein is required for its retention in the Golgi region. J. Cell Biol. 105, 1205–1214.

Mackenzie, J.M., Westaway, E.G., 2001. Assembly and maturation of the flavivirus kunjin virus appear to occur in the rough endoplasmic reticulum and along the secretory pathway, respectively. J. Virol. 75, 10787–10799.

Maeda, J., Maeda, A., Makino, S., 1999. Release of coronavirus E protein in membrane vesicles from virus-infected cells and E protein-expressing cells. Virology 263, 265–272.

Pettersson, R.F., 1991. Protein localization and virus assembly at intracellular membranes. Curr. Top. Microbiol. Immunol. 170, 67–106.

Seemann, J., Jokitalo, E., Pypaert, M., Warren, G., 2000a. Matrix proteins can generate the higher order architecture of the Golgi apparatus. Nature 407, 1022–1026.

Seemann, J., Jokitalo, E.J., Warren, G., 2000b. The role of the tethering proteins p115 and GM130 in transport through the Golgi apparatus in vivo. Mol. Biol. Cell 11, 635–645.

Stern, D.F., Burgess, L., Sefton, B.M., 1982. Structural analysis of virion proteins of the avian coronavirus infectious bronchitis virus. J. Virol. 42, 208–219.

Sturman, L.S., Holmes, K.V., Behnke, J., 1980. Isolation of coronavirus envelope glycoproteins and interaction with the viral nucleocapsid. J. Virol. 33, 449–462.

Swift, A.M., Machamer, C.E., 1991. A Golgi retention signal in a membrane-spanning domain of coronavirus E1 protein. J. Cell Biol. 115, 19–30.

Vennema, H., Godeke, G.J., Rossen, J.W., Voorhout, W.F., Horzinek, M.C., Opstelten, D.J., Rottier, P.J., 1996. Nucleocapsid-independent assembly of coronavirus-like particles by co- expression of viral envelope protein genes. EMBO J 15, 2020–2028.

Weisz, O.A., Machamer, C.E., 1994. Use of recombinant vaccinia virus vectors for cell biology. Methods Cell Biol. 43, 137–159.

Weisz, O.A., Swift, A.M., Machamer, C.E., 1993. Oligomerization of a membrane protein correlates with its retention in the Golgi complex. J. Cell Biol. 122, 1185–1196.